Current Biology 22, 147–153, January 24, 2012 ©2012 Elsevier Ltd All rights reserved DOI 10.1016/j.cub.2011.11.058

Report

An ARF6/Rab35 GTPase Cascade for Endocytic Recycling and Successful Cytokinesis

Laurent Chesneau,[1] Daphné Dambournet,[1,4] Mickaël Machicoane,[1,4] Ilektra Kouranti,[1] Mitsunori Fukuda,[2] Bruno Goud,[3] and Arnaud Echard[1,*]

[1]Membrane Traffic and Cell Division Lab, Institut Pasteur, CNRS URA2582, 25–28 Rue du Docteur Roux, 75015 Paris, France

[2]Laboratory of Membrane Trafficking Mechanisms, Department of Developmental Biology and Neurosciences, Graduate School of Life Sciences, Tohoku University, Aobayama, Aoba-ku, Sendai, Miyagi 980-8578, Japan

[3]Molecular Mechanisms of Intracellular Transport Lab, Institut Curie, CNRS UMR144, 25 Rue d'Ulm, 75005 Paris, France

Summary

Cytokinesis bridge instability leads to binucleated cells that can promote tumorigenesis in vivo [1]. Membrane trafficking is crucial for animal cell cytokinesis [2–8], and several endocytic pathways regulated by distinct GTPases (Rab11, Rab21, Rab35, ARF6, RalA/B) [9–16] contribute to the postfurrowing steps of cytokinesis. However, little is known about how these pathways are coordinated for successful cytokinesis. The Rab35 GTPase controls a fast endocytic recycling pathway and must be activated for SEPTIN cytoskeleton localization at the intercellular bridge, and thus for completion of cytokinesis [12]. Here, we report that the ARF6 GTPase [17, 18] negatively regulates Rab35 activation and hence the Rab35 pathway. Human cells expressing a constitutively activated, GTP-bound ARF6 mutant display identical endocytic recycling and cytokinesis defects as those observed upon overexpression of the inactivated, GDP-bound Rab35 mutant. As a molecular mechanism, we identified the Rab35 GAP EPI64B as an effector of ARF6 in negatively regulating Rab35 activation. Unexpectedly, this regulation takes place at clathrin-coated pits, and activated ARF6 reduces Rab35 loading into the endocytic pathway. Thus, an effector of an ARF protein is a GAP for a downstream Rab protein, and we propose that this hierarchical ARF/Rab GTPase cascade controls the proper activation of a common endocytic pathway essential for cytokinesis.

Results and Discussion

ARF6 and Rab35 GTPases Act Antagonistically in Endocytic Recycling

Small GTPases of the Rab and ARF families are well-established regulators of membrane traffic in eukaryotic cells and are attractive candidates for connecting and coordinating the different endocytic pathways essential for late cytokinesis steps [17–20]. Indeed, (1) they cycle between GDP (inactive) states and GTP (active) states; (2) conversion between states is precisely regulated by interactions with specific activating GEFs (guanine nucleotide exchange factors) and deactivating GAPs (GTPase-activating proteins); and (3) GTP-bound conformers interact with effector proteins that can be shared between connected pathways. We previously reported that human HeLa cells overexpressing the Rab35 S22N mutant (dominant-negative, GDP-bound form of Rab35) are impaired in fast endocytic recycling and accumulate characteristic intracellular vacuoles positive for the PI(4,5)P2 lipid and for F-actin in 18% of the cells ([12]; see also Figure S1A available online). Overexpression of a GTPase-defective mutant of ARF6 (ARF6 Q67L, GTP-bound) also led to accumulation of PI(4,5)P2 and F-actin-positive vacuoles in 20% of the transfected cells (Figure S1A), as already described [21]. This suggested that Rab35-GDP and ARF6-GTP perturbed endocytic recycling in a similar manner, and we hypothesized that Rab35 and ARF6 may regulate the same transport pathway. Confirming this hypothesis, we found that the major histocompatibility complex class I (MHC-I), which is a reported cargo for the ARF6 pathway [22], strongly accumulated on the intracellular vacuoles induced by both ARF6 Q67L and Rab35 S22N (Figure 1A). In addition, the transferrin receptor (TfR), which was known to be enriched on those vacuoles in Rab35 S22N-expressing cells [12], also accumulated on the vacuoles induced by ARF6 Q67L overexpression (Figure 1A). Importantly, fast endocytic recycling of internalized transferrin was strongly reduced both in Rab35 S22N-expressing cells and in ARF6 Q67L-expressing cells (Figure 1B). These vacuoles were not positive for other endocytic markers such as Rab5, EEA1, Rab4, or Rab11 (Figure S1B), indicating that there was not a general or unspecific mixing of all endocytic pathways in these cells. Finally, the cytoskeletal element SEPTIN2, which is known to be associated with PI(4,5)P2 and F-actin, was strongly reduced at the cell cortex and accumulated on the intracellular vacuoles, both in Rab35 S22N [12] and in ARF6 Q67L-expressing cells (Figure 1A). Of note, SEPTIN2 localization on vacuoles was not dependent on F-actin (Figure S1C). Taken together, these results indicate that overactivation of ARF6 and inactivation of Rab35 lead to identical endocytic recycling defects. It also suggests that ARF6 and Rab35 GTPases act antagonistically in a common transport pathway.

ARF6 Acts Upstream of Rab35 and Antagonizes Rab35 Activation in Endocytosis and in Postfurrowing Steps of Cytokinesis

We previously reported that endocytic recycling defects in Rab35 S22N-expressing cells were associated with cytokinesis failures characterized by delocalization of SEPTIN2 to intracellular vacuoles, poor SEPTIN2 enrichment at the intercellular bridge, and thus bridge instability [12]. ARF6 Q67L-expressing cells are known to accumulate binucleated cells, but it is not known at which exact step and for which molecular reason cytokinesis fails [14]. Time-lapse microscopy revealed that cells expressing either Rab35 S22N or ARF6 Q67L mutants entered mitosis normally but failed in cytokinesis after furrow ingression in 20% (n = 158) and 18% (n = 165) of the cells, respectively, as compared to 0.7% (n = 269) in control cells (Figure S2A). Regression of the intercellular bridge was observed 1–5 hr after its formation in both Rab35 S22N- and ARF6 Q67L-expressing cells, leading to binucleated cells. To

[4]These authors contributed equally to this work
*Correspondence: arnaud.echard@pasteur.fr

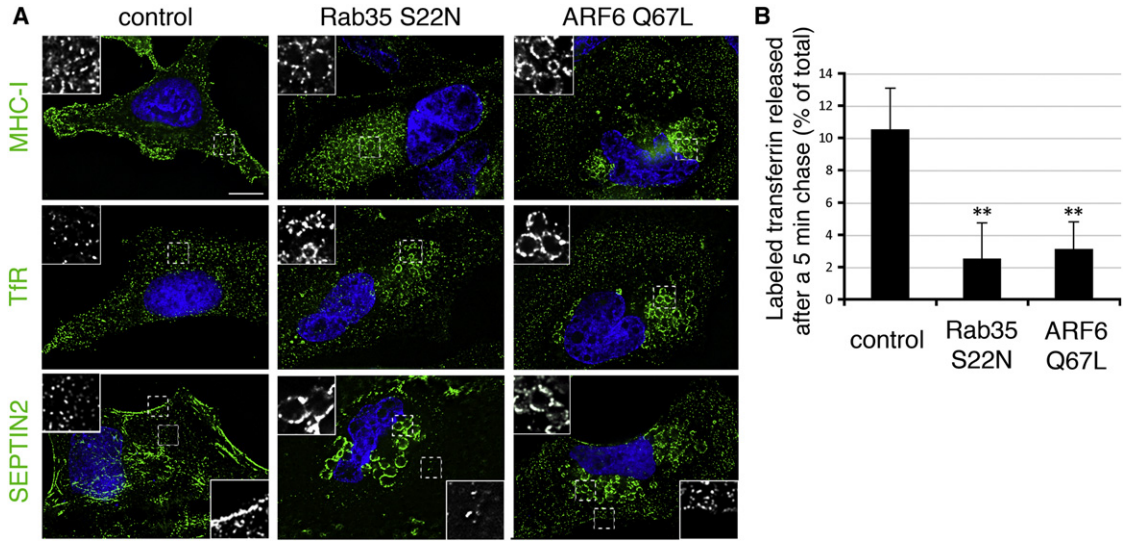

Figure 1. ARF6 and Rab35 Act Antagonistically in Endocytic Recycling

(A) HeLa cells expressing either the GTPase-deficient, active ARF6 Q67L mutant or the dominant-negative, inactive Rab35 S22N mutant were stained for the indicated proteins (green). Blue indicates DAPI staining. Insets show higher magnifications (dashed lines) of intracellular regions (upper left insets) or cortical regions (lower right insets). Scale bar represents 20 μm.

(B) HeLa cells expressing the ARF6 Q67L mutant or the Rab35 S22N mutant were loaded with fluorescently labeled transferrin by continuous uptake at 37°C for 30 min. Fast TfR recycling to the cell surface was measured by quantification of intracellular, labeled transferrin that remained after a 5 min chase at 37°C into a medium containing unlabeled transferrin. The FACS results are expressed as the intracellular fraction of loaded transferrin that was released from cells in each condition (mean ± SEM for four independent experiments, 2,000–3,000 cells analyzed per experiment). $^{**}p < 2.5 \times 10^{-2}$ (Student's t test).

gain insight into the mechanism responsible for bridge instability in ARF6 Q67L-expressing cells, we examined whether SEPTIN2 enrichment, which is required for bridge stability [23], was impaired in dividing cells, as we reported for Rab35 S22N-expressing cells [12]. In ARF6 Q67L-expressing cells, SEPTIN2 was strongly delocalized from ingressing furrows (data not shown) and from the cell cortex of early bridges to intracellular vacuoles (Figure 2A), which accounts at least in part for the observed cytokinesis defects. We conclude that overactivation of the ARF6 GTPase or inactivation of the Rab35 GTPase leads to similar cytokinesis defects characterized by abnormal SEPTIN2 localization and intercellular bridge instability.

We reasoned that if the ARF6 and Rab35 GTPases act antagonistically in the same recycling pathway essential for cytokinesis (Figures 1, S1A, 2A, and S2A), either ARF6-GTP (ARF6 Q67L) acts upstream and induces the conversion of Rab35 to its GDP-bound inactive state (model 1, Figure S2B), or Rab35-GDP (Rab35 S22N) acts upstream and induces the conversion of ARF6 to its GTP-bound active state (model 2, Figure S2B). In agreement with the first scenario, we found that cytokinesis defects observed after ARF6 Q67L overexpression were reduced approximately 2-fold by the coexpression of a constitutively GTP-bound (GTPase-deficient) mutant of Rab35 (Rab35 Q67L) (Figures 2A and 2B). Rab35 Q67L overexpression alone, which does not inhibit endocytic recycling [12], did not perturb cytokinesis either (Figures 2A and 2B). Furthermore, cytokinesis defects induced by Rab35 S22N overexpression were not suppressed by coexpression of a GDP-bound dominant-negative ARF6 mutant (ARF6 T27N, Figure S2C), in contradiction with model 2. Further supporting model 1, and consistent with cytokinesis defects being associated with endocytic defects after ARF6 Q67L overexpression, the number of cells displaying intracellular vacuoles was also reduced after coexpression of the constitutively active Rab35 Q67L mutant (Figure 2C). Importantly, these epistasis experiments were confirmed by directly measuring the levels of activated Rab35, using a recently developed GTP-Rab35 trap [24]. Indeed, we observed that GTP-bound Rab35 levels were strongly reduced in cells that expressed ARF6 Q67L (Figure 2D). Altogether, we conclude that ARF6 acts upstream of Rab35 in the same endocytic recycling pathway important for cytokinesis, and that GTP-bound active ARF6 promotes the conversion of Rab35 into its inactive, GDP-bound state.

EPI64B Is a Rab35 GAP in Both Endocytic Recycling and Cytokinesis

To explore the molecular mechanism implicated in this ARF/Rab cascade, we focused our attention on the members of the EPI64/TBC1D10 protein family (Figure S3A). Indeed, EPI64A, EPI64B, and the immune-specific EPI64C have been shown to display a GAP activity toward the Rab35 GTPase, with Rab35 appearing as the preferred substrate for EPI64B in systematic analysis in vitro [25, 26]. In addition, EPI64C overexpression reduces GTP-bound Rab35 levels in vivo [24]. Interestingly, the overexpression of EPI64A leads to the accumulation of intracellular, F-actin-positive membranes of unknown origin [27], which resemble the F-actin-positive intracellular vacuoles described in Figure S1A. We focused on EPI64B because RT-PCR revealed that EPI64B was the major EPI64 family member expressed in HeLa cells (data not shown).

To test whether EPI64B is a functional Rab35 GAP able to control the Rab35 endocytic pathway and cytokinesis, we first analyzed whether overexpression of the GDP-bound Rab35 S22N mutant and overexpression of EPI64B led to identical endocytic recycling defects. EPI64B overexpression induced

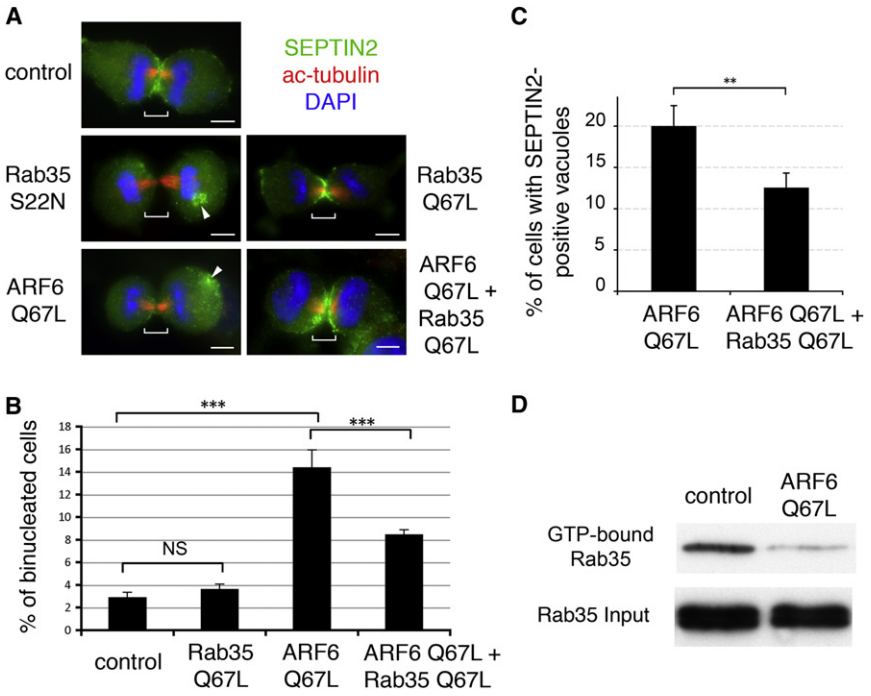

Figure 2. ARF6 Acts Upstream of Rab35 and Antagonizes Rab35 Activation during Both Interphase and Cytokinesis

(A) Dividing HeLa cells expressing the Rab35 S22N mutant or the ARF6 Q67L mutant or the Rab35 Q67L mutant, or coexpressing Rab35 Q67L and ARF6 Q67L were stained for SEPTIN2 (green) when the intercellular bridge was present (labeled by acetyl [ac]-tubulin, red). Blue indicates DAPI staining. Note that SEPTIN2 is strongly delocalized from the bridge region (brackets) to intracellular membranes (arrowheads) in cells expressing the Rab35 S22N mutant or the ARF6 Q67L mutant. Scale bars represent 10 μm.

(B) Number of binucleated cells after transfection with control (empty) plasmid, GTPase-deficient Rab35 Q67L-encoding plasmid, or ARF6 Q67L-encoding plasmid, or after cotransfection with ARF6 Q67L- and Rab35 Q67L-encoding plasmids for 48 hr, mean ± SEM for five independent experiments, 250–450 cells per experiment. ***$p < 8 \times 10^{-3}$ (Student's t test); NS, not significant.

(C) Number of HeLa cells with SEPTIN2-positive intracellular vacuoles after cotransfection either with control (empty) and ARF6 Q67L-encoding plasmids or with ARF6 Q67L- and Rab35 Q67L-encoding plasmids, as indicated. **$p = 4 \times 10^{-2}$ (Student's t test), mean ± SEM for three independent experiments, 100–150 cells analyzed per experiment.

(D) COS7 cells were cotransfected with wild-type Flag-Rab35 and either control or ARF6 Q67L-encoding plasmids for 48 hr. The upper panel indicates the amount of GTP-bound Flag-Rab35 that has been selectively pulled down from each cell lysate (see Supplemental Experimental Procedures). The amount of total (GDP- and GTP-bound) Flag-Rab35 (1% input) in each lysate is presented in the lower panel.

the formation of intracellular vacuoles positive for F-actin, PI(4,5)P2, SEPTIN2, MHC-I, and TfR, as well as a strong reduction of SEPTIN2 at the cell cortex (Figure S3B), as observed in Rab35-GDP mutant-expressing cells (Figures 1A and S1A). These vacuoles were not marked by the Rab4, Rab5, or Rab11 endocytic markers (Figure S3C). Consistent with endocytosis being perturbed, overexpression of EPI64B strongly inhibited the fast recycling of TfR from endosomes to the plasma membrane (Figure S3D), as observed in Rab35 S22N-expressing cells (Figure 1B). Of note, the formation of intracellular vacuoles was dependent on the GAP activity of EPI64B (data not shown). In addition, the presence of intracellular vacuoles in EPI64B-expressing cells was suppressed by the coexpression of the constitutively active, GTP-bound Rab35 Q67L mutant (Figure 3A). Finally, GTP-bound Rab35 levels were strongly reduced in cells expressing EPI64B, but not the GAP-defective mutant EPI64B R409K (Figure 3B), demonstrating that Rab35 was indeed inactivated in EPI64B-expressing cells.

We next analyzed whether the overexpression of EPI64B perturbed cytokinesis. Time-lapse microscopy further supported the role of EPI64B as a Rab35 GAP: cytokinesis failed after furrow ingression in 16% (n = 224) of the EPI64B-expressing cells (Figure S3E), and was associated with a delocalization of SEPTIN2 from the bridge to intracellular membranes (Figure 3C). In addition, cytokinesis failures depended on the GAP activity of EPI64B, because no cytokinesis defects were observed upon overexpression of the catalytically defective mutant EPI64B R409K (Figure 3D). Importantly, the cytokinesis defects (Figures 3C and 3D) in EPI64B-expressing cells were suppressed by the coexpression of the constitutively active, GTP-bound Rab35 Q67L mutant, confirming that Rab35 is the relevant target of EPI64B in vivo.

To further support that EPI64B is a Rab35 GAP, we analyzed whether these two proteins colocalized during endocytosis in interphase and during cytokinesis. We first investigated Rab35 and EPI64B localization in interphase cells, because cytokinesis defects are likely a consequence of interphase endocytic defects. Indeed, abnormal endocytic recycling in interphase led to the formation of intracellular vacuoles (Figures 1A and S3B) that were still present and positive for SEPTIN2 during mitosis (arrowheads, Figures 2A and 3C). In addition, time-lapse microscopy indicated that cells containing vacuoles prior to mitosis displayed cytokinesis defects (data not shown). Altogether, this is consistent with cytokinesis defects being a consequence of the delocalization of SEPTIN2 from the cell cortex to intracellular membranes before cell division in Rab35 S22N-, EPI64B-, and ARF6 Q67L-expressing cells. Using immunoelectron microscopy, we reported that Rab35 is localized at the plasma membrane and in clathrin-coated pits, as well as in internal endosomes in interphase [12]. This has been confirmed in fixed cells using immunocytochemistry in mammalian cells and *C. elegans* [28, 29], but the fraction of clathrin-coated pits loaded with Rab35 and the dynamics of Rab35 in these structures were unknown. In addition, EPI64 family members have been described at the plasma membrane, but no detailed localization has been reported [25–27]. Using total internal reflection fluorescence (TIRF) microscopy on living HeLa cells coexpressing wild-type GFP-Rab35 and dsRed-clathrin light chain (CLC), Rab35 was found to colocalize with CLC-positive spots at the plasma membrane, corresponding to either clathrin-coated pits or clathrin-coated platforms from which vesicles bud (Figure 3E). Only a fraction of CLC-positive spots (8.4% ± 0.6%, mean ± SEM, 7,744 CLC-positive spots analyzed) was labeled by Rab35 during the recording of 1 min movies, with Rab35

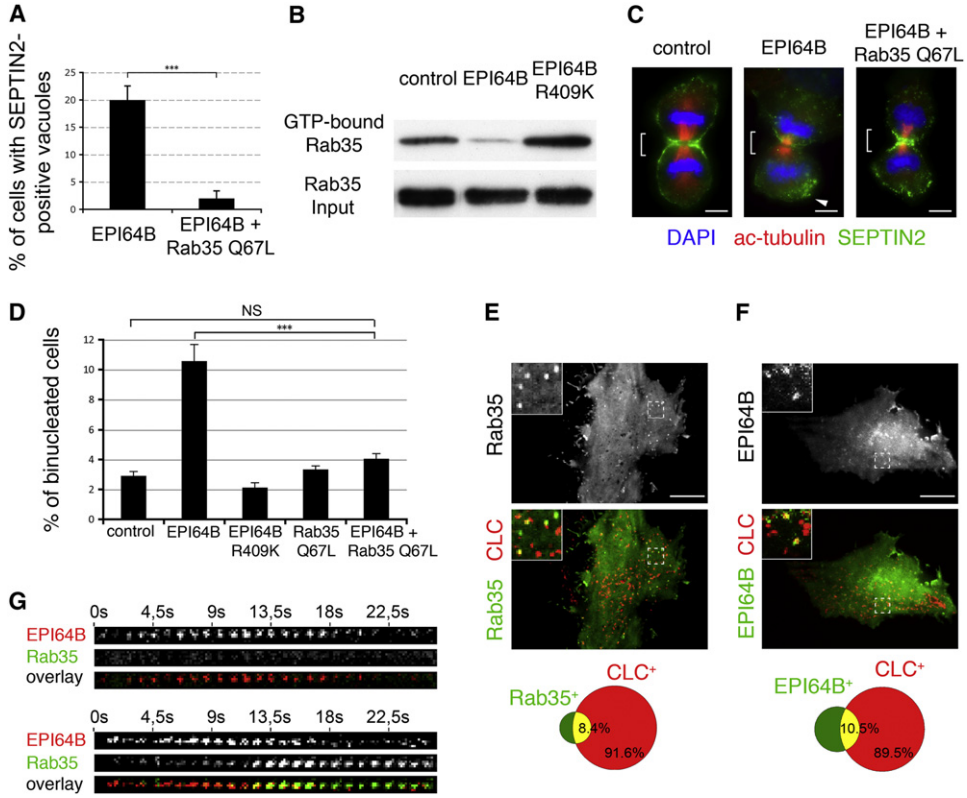

Figure 3. EPI64B Is a Rab35 GAP during Interphase and Cytokinesis and Transiently Colocalizes with Rab35 at the Plasma Membrane in Clathrin-Coated Structures

(A) Number of HeLa cells with SEPTIN2-positive intracellular vacuoles after cotransfection either with control (empty) and EPI64B-encoding plasmids, or with EPI64B- and Rab35 Q67L-encoding plasmids, as indicated. ***$p = 1.6 \times 10^{-3}$ (Student's t test), mean ± SEM for three independent experiments, 50–150 cells analyzed per experiment.

(B) The amount of GTP-bound Flag-tagged Rab35 in cell lysates expressing control (empty), EPI64B-, or GAP-deficient EPI64B R409K-encoding plasmids was analyzed as in Figure 2D.

(C) SEPTIN2 localization (green) in dividing cells transfected with control (empty) or EPI64B-encoding plasmids, or cotransfected with EPI64B and Rab35 Q67L-encoding plasmids (see also Figure 2A). Scale bars represent 10 μm.

(D) Number of binucleated cells after transfection with control (empty) plasmid, EPI64B- or GAP-deficient R409K EPI64B mutant-encoding plasmids, or Rab35 Q67L-encoding plasmid, or after cotransfection with EPI64B- and Rab35 Q67L-encoding plasmids for 48 hr, mean ± SEM for four independent experiments, 300–400 cells per experiment. ***$p = 5 \times 10^{-3}$ (Student's t test); NS, not significant.

(E) HeLa cells cotransfected with GFP-tagged wild-type Rab35 (displayed in green) and dsRedFP-tagged CLC (displayed in red) were recorded by time-lapse TIRF microscopy. Upper panel shows a temporal projection of a representative 1 min movie. Inset shows the indicated regions (dashed line) at higher magnification. Scale bar represents 10 μm. Lower panel shows quantification of Rab35/CLC colocalization in 1 min movies (n = 7,744 clathrin-coated spots analyzed).

(F) HeLa cells cotransfected with cherryFP-tagged EPI64B (displayed in green) and GFP-tagged CLC (displayed in red) were analyzed and quantified as described in (E) (n = 2,228 clathrin-coated spots analyzed). Scale bar represents 10 μm.

(G) HeLa cells were cotransfected with GFP-tagged wild-type Rab35 (green) and cherryFP-tagged EPI64B (red). Snapshots of representative time-lapse TIRF microscopy image series are displayed. Either EPI64B spots appear and disappear without Rab35 labeling (upper panels, 85% of the cases) or Rab35 appears when EPI64B staining decreases (lower panels, 15% of cases; n = 680 EPI64B spots analyzed).

always arriving after clathrin (Figure 3E). In addition, 10.5% ± 3.5% (2,228 CLC-positive spots analyzed) of the CLC-positive spots became positive for EPI64B during the recording of 1 min movies (Figure 3F). When we examined the relative dynamics of EPI64B and Rab35, the majority of EPI64B spots appeared and disappeared without any Rab35 labeling (85% ± 1.8%, 680 EPI64B-positive spots analyzed; Figure 3G, upper panel). Strikingly, in 15% of EPI64B spots, Rab35 appeared and accumulated only when EPI64B decreased from a given spot at the plasma membrane (Figure 3G, lower panel). Importantly, we never observed a Rab35 spot that later became positive for EPI64B. These observations indicate that EPI64B and Rab35 transiently colocalize in CLC-positive structures at the plasma membrane. In addition it strongly suggests that EPI64B controls Rab35 association to CLC-positive structures by limiting Rab35 activation at early steps of endocytosis (see also below). Of note, the dynamics and localization of Rab35 and EPI64B in CLC-positive structures at the plasma membrane were confirmed in cells during cytokinesis (Figure S3F). Altogether, we conclude that EPI64B is a functional RabGAP that specifically converts Rab35 into its GDP state, and that there is a tight temporal control of EPI64B/Rab35 localization in CLC-positive structures.

GTP-Bound ARF6 Interacts with EPI64B and Negatively Regulates Rab35 Activation in Clathrin-Coated Structures

Because we identified EPI64B as the relevant RabGAP for Rab35 in both endocytic recycling and cytokinesis, we next

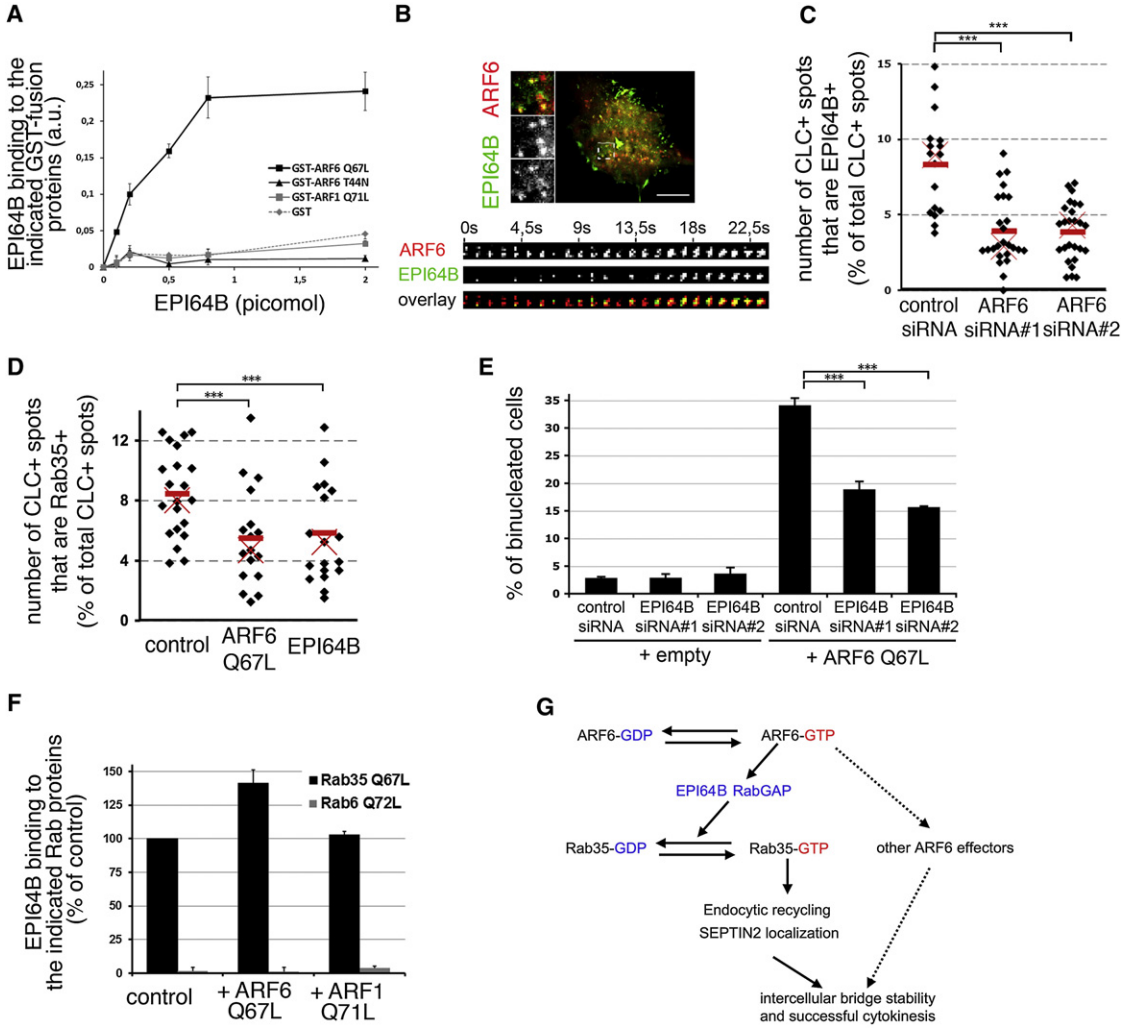

Figure 4. GTP-Bound ARF6 Interacts Directly with EPI64B and Negatively Regulates Rab35 Activation in Clathrin-Coated Structures

(A) Binding of recombinant hexahistidine-tagged EPI64B (aa 1–650) to indicated recombinant GST, GST-ARF6 Q67L, GST-ARF6 T44N, or GST-ARF1 Q71L (mean ± SEM, n = 3 experiments).

(B) HeLa cells were cotransfected with cherryFP-EPI64B (displayed in green) and GFP-tagged wild-type ARF6 (displayed in red). Temporal projection and snapshots of a representative 1 min time-lapse TIRF microscopy movie are displayed. Scale bar represents 10 μm.

(C) HeLa cells treated with either control or two independent ARF6 siRNAs for 3 days were then cotransfected with cherryFP-tagged EPI64B and GFP-tagged CLC for 24 hr. Cells were recorded by time-lapse TIRF microscopy for 1 min movies. The percentage of CLC-positive spots that were positive for EPI64B is displayed for each analyzed cell (diamonds). Median (red cross) and mean (red bar) of the distribution are indicated. A total of 2,700–5,000 clathrin-coated structures were analyzed. ***$p < 4 \times 10^{-5}$ (Student's t test).

(D) HeLa cells expressing both GFP-tagged wild-type Rab35 and dsRedFP-CLC were cotransfected with either control, EPI64B-, or ARF6 Q67L-encoding plasmids. Cells were recorded by time-lapse TIRF microscopy, and quantification of Rab35/CLC colocalization in 1 min movies in each condition is displayed (n > 5,000 clathrin-coated structures analyzed per condition). ***$p < 9 \times 10^{-3}$ (Student's t test).

(E) HeLa cells treated with either control or two independent EPI64B siRNAs for 2 days were then transfected with control (empty) or with the HA-tagged ARF6 Q67L mutant-encoding plasmid. The number of HA-positive, binucleated cells was quantified 48 hr after the plasmid transfection (mean ± SEM, n = 3 independent experiments, 400 cells per experiment). ***$p < 3 \times 10^{-3}$ (Student's t test).

(F) Binding of recombinant hexahistidine-tagged EPI64B (aa 1–650) to recombinant untagged Rab35 Q67L (as in A) (black bars), in the presence of GST-tagged ARF6 Q67L or GST-tagged ARF1 Q71L. Rab6 Q72L was used as a negative control (gray bars) (mean ± SEM, n = 4 experiments). ***$p = 3.4 \times 10^{-3}$ (Student's t test).

(G) Proposed molecular model for the ARF6/Rab35 cascade regulating Rab35 activation in endocytosis and cytokinesis.

tested whether EPI64B is involved in the ARF6/Rab35 cascade we describe. So far, EPI64A has been shown to interact with the GTP-bound form of the ARF6 GTPase [27], which raises the possibility that other members of this family could also bind to activated ARF6. This would provide a molecular mechanism explaining how ARF6-GTP inhibits Rab35 activation. Two-hybrid experiments indicated that full-length EPI64B interacted with the GTP-bound (ARF6 Q67L) but not with the GDP-bound (ARF6 T27N) mutant of ARF6 (data not shown). In addition, recombinant EPI64B (aa 1–650) was able to bind in a dose-dependent manner with purified ARF6 Q67L, but not ARF6 T44N or ARF1 Q71L (Figure 4A). This demonstrates that EPI64B directly interacts with GTP-bound ARF6. Consistent with this interaction, ARF6 and EPI64B colocalized in

CLC-positive spots at the plasma membrane. TIRF microscopy analysis revealed that 98.9% ± 0.8% of the ARF6-positive spots were positive for CLC (1,484 clathrin-positive structures analyzed), an observation that was also recently reported in HeLa cells and BSC-1 cells [30]. Of note, we observed that wild-type ARF6 and ARF6 Q67L always preceded EPI64B appearance at CLC-positive spots, suggesting that ARF6 could recruit EPI64 in these structures (Figures 4B and S4A). Consistent with this hypothesis, the number of CLC-positive spots that were EPI64B-positive was reduced after ARF6 depletion by RNAi, a result that was confirmed with two independent siRNAs (3,500–4,000 clathrin spots analyzed; Figures 4C and S4B). In addition, colocalization between ARF6 and EPI64B was also observed during cytokinesis (Figure S4C). Thus, GTP-bound ARF6 interacts with EPI64B, and ARF6 is important for the proper localization of EPI64B in CLC-positive structures.

Because both EPI64B and ARF6 partially overlap with Rab35 (Figures 3G, S3F, S4D, and S4E), we next investigated whether the overexpression of the GTP-bound ARF6 mutant or the overexpression of EPI64B could perturb Rab35 association to CLC-positive structures. Indeed, contrary to the GTP-bound Rab35 Q67L mutant, the GDP-bound Rab35 S22N mutant was not detected in CLC-positive structures (data not shown), suggesting that only activated Rab35 could enter the clathrin-dependent endocytic pathway. TIRF microscopy revealed that the mean number of CLC-positive spots in which Rab35 was loaded was reduced after either EPI64B or ARF6 Q67L overexpression (5,000–8,000 clathrin spots analyzed; Figure 4D). This is consistent with EPI64B being a functional Rab35 GAP that controls Rab35 activation in CLC-positive structures, and with the epistasis experiments placing ARF6 upstream of Rab35 and inhibiting Rab35 activation (Figure 2). To test the contribution of EPI64B in this ARF6/Rab35 cascade, we next analyzed whether the endocytic and cytokinesis defects associated with ARF6 overactivation were reduced in EPI64B-depleted cells, using two independent siRNAs (Figure S4F). Following EPI64B depletion, the number of cells with vacuoles (Figure S4G) and the cytokinesis failures induced by the overexpression of ARF6 Q67L were indeed reduced (Figure 4E). These results indicate that the endocytic and the cytokinesis defects resulting from the overactivation of the ARF6 pathway are, at least in part, dependent on the presence of the Rab35 GAP EPI64B. Interestingly, we found that EPI64B binds to Rab35 in a dose-dependent manner (Figure S4H), and that this interaction was increased by >40% in the presence of GTP-bound ARF6 (Figure 4F). This suggests that the presence of GTP-bound ARF6 at CLC structures favors both EPI64B recruitment and the interaction with its target Rab35. Altogether, we conclude that EPI64B functions downstream of ARF6-GTP and that EPI64B is an ARF6 effector that regulates Rab35 activation.

In this report, we describe an original cascade of two GTPases from different families that control the activation of a common recycling pathway required for successful cytokinesis. We found that ARF6 acts upstream of Rab35 and that ARF6-GTP negatively regulates the activation of Rab35 through the Rab35 GAP EPI64B (Figure 4G). We propose that the overactivation of the ARF6 GTPase inhibits loading of Rab35 in the endocytic pathway. As a consequence, this perturbs endocytic recycling, delocalizes SEPTIN2 cytoskeleton elements from the cell cortex to intracellular vacuoles, and hence induces cytokinesis failure. Thus, ARF6 activation must be precisely regulated for successful cytokinesis, because ARF6 overactivation leads to intercellular bridge instability whereas ARF6 inactivation leads to later penetrant abscission defects [14, 15]. Overactivation of ARF6 has been reported to inhibit several other key cellular functions (such as cell migration, Ca^{2+}-dependent exocytosis, tumor growth) and to promote cancer metastasis and invasiveness, through various effectors and pathways [17]. In light of the present results, it should thus be important to reconsider whether those defects could be, at least in part, attributed to the inhibition of the Rab35-recycling pathway itself. Finally, this antagonistic ARF/Rab cascade may represent a general mechanism for regulating the sequential activation of Rab GTPases in a transport pathway. Indeed, the notion of "Rab cascade" recently emerged, whereby successive Rab GTPases recruit the GEFs and GAPs of other GTPases belonging to the same pathway [19, 20, 31–33]. In particular, in a transport step between two successive compartments, a Rab GTPase on the second compartment terminates the activation of a Rab GTPase characteristic of the first compartment by recruiting the corresponding RabGAP [33]. Here, we propose a complementary and reciprocal mechanism of regulation: a GTPase of the first compartment (in this case an ARF GTPase) prevents the precocious activation of the second Rab GTPase by recruiting the corresponding RabGAP. This mutual inhibition, based on RabGAPs, constitutes a switch, which ensures that each GTPase is active on a particular compartment. Interestingly, it has been reported that GTP-bound Rab35 also interacts with an ARF6 GAP [34] that would be an exact counterpart of the cascade described here. In addition, our results indicate that Rab35 loading into the endocytic pathway depends on a balance between Rab35 GAP and Rab35 GEF, because overexpression of Rab35 S22N (which acts as a dominant negative by sequestrating Rab35 GEFs) inhibited wild-type Rab35 localization in CLC-positive structures (data not shown). Thus, recruitment or activation of a specific Rab35 GEF at CLC-positive structures would contribute to flip the switch and to promote vectorial transport in a trafficking pathway.

Supplemental Information

Supplemental Information includes four figures and Supplemental Experimental Procedures and can be found with this article online at doi:10.1016/j.cub.2011.11.058.

Acknowledgments

We thank P. Chavrier and G. Montagnac for kindly providing reagents, for helpful discussions, and for sharing unpublished data. We thank T. Balla, P. Benaroch, A. Benmerah, M. Franco, A. el Marjou, S. Moutel, F. Perez, and W. Trimble for kindly providing reagents; S. Lodeho for initial plasmid constructions; and S. Miserey-Lenkei and E. Crowell for critical reading of the manuscript. The authors acknowledge the Plate-Forme Production d'Anticorps Recombinants-Institut Curie for antibodies, and the Plate-Forme d'Imagerie Dynamique of the Institut Pasteur and the Nikon Imaging Centre at Institut Curie-CNRS for microscopes, assistance, and excellent support. This work has been supported by the Institut PASTEUR (G5 program), the CNRS, the Agence Nationale pour la Recherche (ANR ANR07-JCJC-0089 to A.E.), the Schlumberger Foundation for Education and Research (to A.E.), and the Institut Curie. M.M. and D.D. have been supported by the Ministère de la Recherche et de l'Enseignement Supérieur and by the Ecole Doctorale Complexité du Vivant. L.C. and D.D. have been supported by the Association pour la Recherche sur le Cancer.

Received: November 24, 2010
Revised: October 31, 2011
Accepted: November 28, 2011
Published online: January 5, 2012

References

1. Fujiwara, T., Bandi, M., Nitta, M., Ivanova, E.V., Bronson, R.T., and Pellman, D. (2005). Cytokinesis failure generating tetraploids promotes tumorigenesis in p53-null cells. Nature *437*, 1043–1047.
2. Glotzer, M. (2001). Animal cell cytokinesis. Annu. Rev. Cell Dev. Biol. *17*, 351–386.
3. Eggert, U.S., Mitchison, T.J., and Field, C.M. (2006). Animal cytokinesis: from parts list to mechanisms. Annu. Rev. Biochem. *75*, 543–566.
4. Montagnac, G., Echard, A., and Chavrier, P. (2008). Endocytic traffic in animal cell cytokinesis. Curr. Opin. Cell Biol. *20*, 454–461.
5. Prekeris, R., and Gould, G.W. (2008). Breaking up is hard to do—membrane traffic in cytokinesis. J. Cell Sci. *121*, 1569–1576.
6. Echard, A. (2008). Membrane traffic and polarization of lipid domains during cytokinesis. Biochem. Soc. Trans. *36*, 395–399.
7. Steigemann, P., and Gerlich, D.W. (2009). Cytokinetic abscission: cellular dynamics at the midbody. Trends Cell Biol. *19*, 606–616.
8. Echard, A., Hickson, G.R., Foley, E., and O'Farrell, P.H. (2004). Terminal cytokinesis events uncovered after an RNAi screen. Curr. Biol. *14*, 1685–1693.
9. Wilson, G.M., Fielding, A.B., Simon, G.C., Yu, X., Andrews, P.D., Hames, R.S., Frey, A.M., Peden, A.A., Gould, G.W., and Prekeris, R. (2005). The FIP3-Rab11 protein complex regulates recycling endosome targeting to the cleavage furrow during late cytokinesis. Mol. Biol. Cell *16*, 849–860.
10. Fielding, A.B., Schonteich, E., Matheson, J., Wilson, G., Yu, X., Hickson, G.R., Srivastava, S., Baldwin, S.A., Prekeris, R., and Gould, G.W. (2005). Rab11-FIP3 and FIP4 interact with Arf6 and the exocyst to control membrane traffic in cytokinesis. EMBO J. *24*, 3389–3399.
11. Pellinen, T., Tuomi, S., Arjonen, A., Wolf, M., Edgren, H., Meyer, H., Grosse, R., Kitzing, T., Rantala, J.K., Kallioniemi, O., et al. (2008). Integrin trafficking regulated by Rab21 is necessary for cytokinesis. Dev. Cell *15*, 371–385.
12. Kouranti, I., Sachse, M., Arouche, N., Goud, B., and Echard, A. (2006). Rab35 regulates an endocytic recycling pathway essential for the terminal steps of cytokinesis. Curr. Biol. *16*, 1719–1725.
13. Dambournet, D., Machicoane, M., Chesneau, L., Sachse, M., Rocancourt, M., El Marjou, A., Formstecher, E., Salomon, R., Goud, B., and Echard, A. (2011). Rab35 GTPase and OCRL phosphatase remodel lipids and F-actin for successful cytokinesis. Nat. Cell Biol. *13*, 981–988.
14. Schweitzer, J.K., and D'Souza-Schorey, C. (2002). Localization and activation of the ARF6 GTPase during cleavage furrow ingression and cytokinesis. J. Biol. Chem. *277*, 27210–27216.
15. Montagnac, G., Sibarita, J.B., Loubéry, S., Daviet, L., Romao, M., Raposo, G., and Chavrier, P. (2009). ARF6 Interacts with JIP4 to control a motor switch mechanism regulating endosome traffic in cytokinesis. Curr. Biol. *19*, 184–195.
16. Cascone, I., Selimoglu, R., Ozdemir, C., Del Nery, E., Yeaman, C., White, M., and Camonis, J. (2008). Distinct roles of RalA and RalB in the progression of cytokinesis are supported by distinct RalGEFs. EMBO J. *27*, 2375–2387.
17. D'Souza-Schorey, C., and Chavrier, P. (2006). ARF proteins: roles in membrane traffic and beyond. Nat. Rev. Mol. Cell Biol. *7*, 347–358.
18. Grant, B.D., and Donaldson, J.G. (2009). Pathways and mechanisms of endocytic recycling. Nat. Rev. Mol. Cell Biol. *10*, 597–608.
19. Grosshans, B.L., Ortiz, D., and Novick, P. (2006). Rabs and their effectors: achieving specificity in membrane traffic. Proc. Natl. Acad. Sci. USA *103*, 11821–11827.
20. Stenmark, H. (2009). Rab GTPases as coordinators of vesicle traffic. Nat. Rev. Mol. Cell Biol. *10*, 513–525.
21. Brown, F.D., Rozelle, A.L., Yin, H.L., Balla, T., and Donaldson, J.G. (2001). Phosphatidylinositol 4,5-bisphosphate and Arf6-regulated membrane traffic. J. Cell Biol. *154*, 1007–1017.
22. Eyster, C.A., Higginson, J.D., Huebner, R., Porat-Shliom, N., Weigert, R., Wu, W.W., Shen, R.F., and Donaldson, J.G. (2009). Discovery of new cargo proteins that enter cells through clathrin-independent endocytosis. Traffic *10*, 590–599.
23. Estey, M.P., Di Ciano-Oliveira, C., Froese, C.D., Bejide, M.T., and Trimble, W.S. (2010). Distinct roles of septins in cytokinesis: SEPT9 mediates midbody abscission. J. Cell Biol. *191*, 741–749.
24. Fukuda, M., Kobayashi, H., Ishibashi, K., and Ohbayashi, N. (2011). Genome-wide investigation of the Rab binding activity of RUN domains: development of a novel tool that specifically traps GTP-Rab35. Cell Struct. Funct. *36*, 155–170.
25. Fuchs, E., Haas, A.K., Spooner, R.A., Yoshimura, S., Lord, J.M., and Barr, F.A. (2007). Specific Rab GTPase-activating proteins define the Shiga toxin and epidermal growth factor uptake pathways. J. Cell Biol. *177*, 1133–1143.
26. Patino-Lopez, G., Dong, X., Ben-Aissa, K., Bernot, K.M., Itoh, T., Fukuda, M., Kruhlak, M.J., Samelson, L.E., and Shaw, S. (2008). Rab35 and its GAP EPI64C in T cells regulate receptor recycling and immunological synapse formation. J. Biol. Chem. *283*, 18323–18330.
27. Hanono, A., Garbett, D., Reczek, D., Chambers, D.N., and Bretscher, A. (2006). EPI64 regulates microvillar subdomains and structure. J. Cell Biol. *175*, 803–813.
28. Sato, M., Sato, K., Liou, W., Pant, S., Harada, A., and Grant, B.D. (2008). Regulation of endocytic recycling by C. elegans Rab35 and its regulator RME-4, a coated-pit protein. EMBO J. *27*, 1183–1196.
29. Allaire, P.D., Marat, A.L., Dall'Armi, C., Di Paolo, G., McPherson, P.S., and Ritter, B. (2010). The Connecdenn DENN domain: a GEF for Rab35 mediating cargo-specific exit from early endosomes. Mol. Cell *37*, 370–382.
30. Montagnac, G., de Forges, H., Smythe, E., Gueudry, C., Romao, M., Salamero, J., and Chavrier, P. (2011). Decoupling of activation and effector binding underlies ARF6 priming of fast endocytic recycling. Curr. Biol. *21*, 574–579.
31. Rink, J., Ghigo, E., Kalaidzidis, Y., and Zerial, M. (2005). Rab conversion as a mechanism of progression from early to late endosomes. Cell *122*, 735–749.
32. Del Conte-Zerial, P., Brusch, L., Rink, J.C., Collinet, C., Kalaidzidis, Y., Zerial, M., and Deutsch, A. (2008). Membrane identity and GTPase cascades regulated by toggle and cut-out switches. Mol. Syst. Biol. *4*, 206.
33. Rivera-Molina, F.E., and Novick, P.J. (2009). A Rab GAP cascade defines the boundary between two Rab GTPases on the secretory pathway. Proc. Natl. Acad. Sci. USA *106*, 14408–14413.
34. Kanno, E., Ishibashi, K., Kobayashi, H., Matsui, T., Ohbayashi, N., and Fukuda, M. (2010). Comprehensive screening for novel rab-binding proteins by GST pull-down assay using 60 different mammalian Rabs. Traffic *11*, 491–507.